Research Paper

A record of change in oyster environment through high-resolution geochemical analysis of Late-Holocene sediments from Coastal Ghana

The Holocene
1–13

DOI: 10.1177/09596836241254483
journals.sagepub.com/home/hol
Sage

Edem Mahu,[1] Melanie J Leng,[2,3] Luke Andrews,[4,5] Apichaya Englong[6] and Robert Marchant[4]

Abstract

The near-coast environments where oysters occur are among the most impacted by humans globally, especially during the Late-Holocene. Yet, in West Africa, there is no documented historical record of change in these environments. We provide insight into the changing geochemical conditions of two oyster environments through high-resolution analysis of total organic carbon (C), total nitrogen (N), carbon and nitrogen isotope ratios ($\delta^{13}C$, $\delta^{15}N$), and trace elements, in two cores retrieved from the Densu estuary and the Anyanui (Keta) Creek in Ghana. Drastic shifts in sedimentation rate occurred in the Keta and Densu cores around 1996 CE and 960 CE respectively. At these times, comparatively, low levels of C and N were found in the Densu core. Increasing C and N levels and decreasing $\delta^{13}C$ upcore aligned with the observed shift in sedimentation rate in the Keta core. The C/N ratios in the Keta core suggest allochthonous organic matter (OM) dominance in the creek. The Densu core showed periodic changes in C/N ratios from very high values (>20) between 1918 BCE and 1321 BCE, to values between 20 and 11 between 1321 BCE and 1977 CE and below 10 from the late 1970s CE to the present day, suggesting a varying degree of transformation in the catchment basin. Extremely high Sulfur (S) and moderate to significant Iron (Fe) increases suggest reducing conditions in the Keta sediments. Moderate Calcium (Ca), Zinc (Zn), and Strontium (Sr) concentrations in the upper part of the Densu core suggest a stronger influence of marine processes in the Densu in recent times. The findings reflect the impacts of catchment basin modification on the health of the two coastal environments, likely to impact the growth, productivity, and sustainability of the fishery of the West African mangrove Oyster.

Keywords

land-use/landcover change, marine processes, organic matter, oyster fishery, reduction processes, sedimentation, sustainability

Received 10 October 2023; revised manuscript accepted 11 April 2024

Introduction

Oyster fisheries contribute significantly to the well-being and livelihood needs of artisanal coastal communities in West Africa (Mahu et al., 2022). For many years, the oyster fishery, dominated by women, has sustained vulnerable communities across coastal West Africa and continues to remain relevant in the context of food security, poverty alleviation, health, and well-being, and supporting gender balance. All these factors contribute directly to attaining the UN Sustainable Development Goals. Within the context of ecosystem systems services, oysters contribute significantly to improving environmental health, protecting coastlines, and mitigating climate change, thus featuring significantly in the goals of the United Nations Ocean decade for sustainable development (2021–2030). Despite these numerous societal and ecosystem benefits, oyster populations have declined globally due to various anthropogenic pressures (Zu Ermgassen et al., 2020). More than 85% of oyster reefs have been lost to habitat degradation, water quality impairment, climate change, and mangrove deforestation, ranking them among the most threatened ecosystems on our planet today (Beck et al., 2011).

Oyster environments comprise nearshore ecosystems such as estuaries, lagoons, and mangrove ecosystems. These environments are highly dynamic but also complex and challenging due to constantly changing conditions (Montagna et al., 2012). Large variations in geochemical conditions often driven by catchment area modifications profoundly affect oyster growth, reproduction, productivity, and survival (North et al., 2010). Landcover removal and other land use changes accelerate the influx of sediments, organic matter, nitrogen, and trace elements to such transitional

[1]Department of Marine and Fisheries Sciences, University of Ghana, Accra, Ghana
[2]British Geological Survey, Keyworth, Nottingham, UK
[3]School of Biosciences, University of Nottingham, Loughborough, UK
[4]Department of Environment and Geography, University of York, York, North Yorkshire, UK
[5]Climate Change Ecology Research Unit, Faculty of Geographical and Geological Sciences, Adam Mickiewicz University, Poznan, Poland
[6]Biological Sciences Program, Department of Botany, Chulalongkorn University, Bangkok, Thailand

Corresponding author:
Edem Mahu, Department of Marine and Fisheries Sciences, University of Ghana, PO BOX LG 99, Accra, Ghana.
Email: emahu@ug.edu.gh

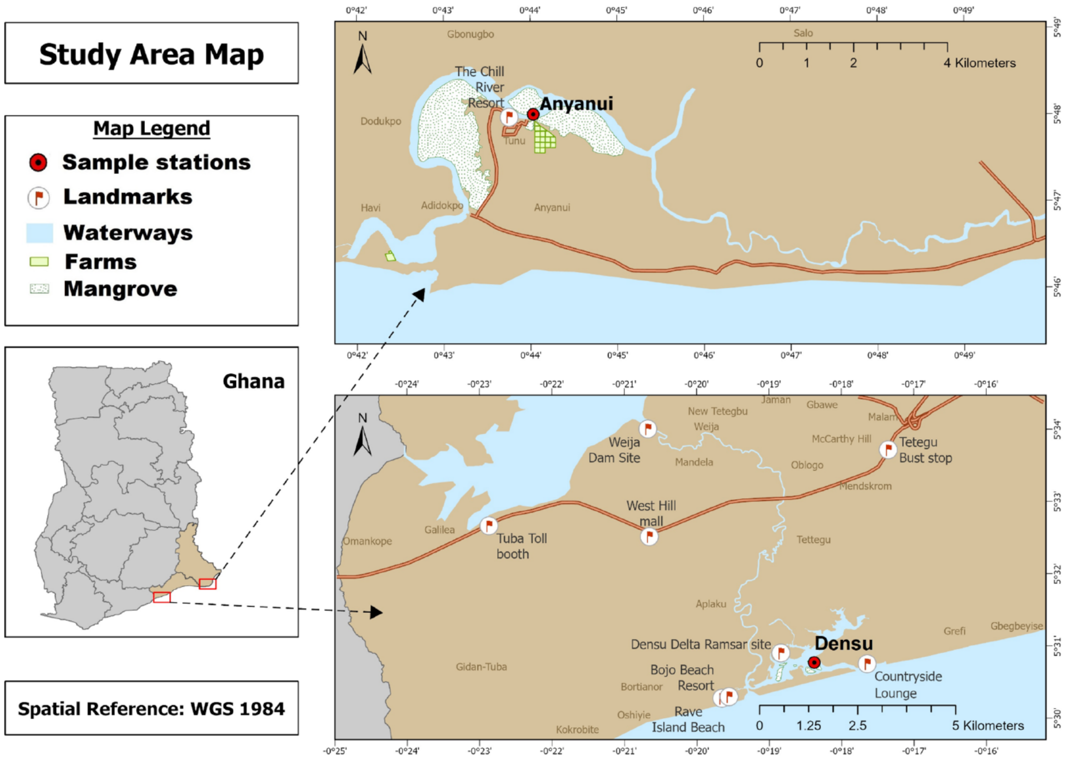

Figure 1. Map of sampling areas in the Densu Estuary and the Anyanui Creek, Ghana.

environments, thereby, altering their natural cycling, and creating undesirable impacts on the ecosystem (Kennish, 2002). While the flux of organic matter into coastal ecosystems is important for food web dynamics and productivity (Bernoux et al., 1998), an excessive supply of organic matter could compromise estuarine health. For instance, marine primary production typically removes CO_2 from surface water, thereby decreasing ocean acidification, and adding this carbon as organic matter to bottom waters (Capelle et al., 2020). Microbial breakdown of organic matter in bottom waters releases CO_2, consequently lowering the bottom water pH (Hopkinson et al., 1998). Notably, carbon cycling in the marine environment promotes aragonite under-saturation and pCO_2 elevation everywhere except in surface waters, with the most significant impacts in bottom waters (Capelle et al., 2020). For bottom-dwelling shellfish such as oysters, a lower aragonite under-saturation state results in difficulties in shell building, leading to shell thinning, reduced growth rate, and increased mortality (Gazeau et al., 2011). Another consequence of high organic matter levels is the removal of dissolved oxygen through microbial respiration (Wallace et al., 2014), resulting in low dissolved oxygen levels. Stress from low dissolved oxygen can yield profound lethal and sublethal effects on many species, including oysters, leading to reduced growth, reduced feeding, and increased susceptibility to disease (Baker and Mann, 1994; David et al., 2005; Patterson et al., 2014).

The C/N ratios allow source determination of organic matter in estuarine ecosystems, providing insight into how much influence estuaries and other nearshore coastal ecosystems receive from fluvial or marine processes (Perdue and Koprivnjak, 2007). Typically, C/N ratios between 4 and 10 indicate dominant marine influence or in-estuary productivity, whereas ratios greater than 20 depict largely fluvial processes and terrestrial organic matter influx into coastal ecosystems (Andersson et al., 2012). The $\delta^{13}C$ and $\delta^{15}N$ reflect both salinity and productivity variabilities in coastal ecosystems, thereby, helping to discriminate between fluvial and marine processes (Medina and Francisco, 1997). Salinity is an important ecological factor in oyster growth and health. Changes in salinity have profound effects on the physiology of oysters including altered filtration and respiration rates, growth, reproduction, and mortality (Sutton et al., 2012; Yankson, 1990). Estimates of C/N ratios combined with $\delta^{13}C$ and $\delta^{15}N$ are important proxies for understanding historical changes in salinity and nutrient regimes in oyster environments while deepening our understanding of the impacts of watershed hydrological modifications on the environmental health of oysters and the fisheries surrounding these (Leng and Lewis, 2017).

While the health of oyster environments globally has been reported to be on the decline, the availability of historical data on how these environments in West Africa have changed is unknown due to limited research. High-resolution, long-term historical data on estuarine geochemistry do not exist. This paucity of estuarine biogeochemical data constrains our understanding of what is changing in oyster environments, the extent and magnitude of the change, and possible consequences to livelihoods and ecosystem services. The present study used variabilities in trace elements (Al, Si, K, Ti, Ca, Fe, Rb, Zn, Sr, Zr, Mn), C and N, (C/N ratios), $\delta^{13}C$, and $\delta^{15}N$ to look for geochemical changes in oyster environments in Ghana over the past ~3000 years. Although the data presented has wider implications for coastal ecosystem health, this paper will discuss findings in relation to oyster health and productivity in West Africa.

Materials and methods

Sediment coring and preparation

Two sediment cores 150 and 200 cm in length were retrieved in December 2021 from the mouth of the Densu Estuary (Densu core) and Keta-Anyanui Creek (Keta core) respectively (Figure 1) Located in the urbanized region of Ghana's capital, the Densu Estuary connects the Densu River to the Atlantic Ocean and supports healthy populations of the West African Mangrove Oyster *Crassotrea tulipa*. Due to its location, the Densu estuary, a Ramsar site, has experienced significant historical land-use and land cover changes in its catchment, with significant growth in the built-up environment (Frank et al., 2019). The Anyanui Creek, a tributary of the Volta estuary connects the Volta River, the Keta Lagoon, and the Atlantic Ocean. The Creek is situated in a dense mangrove forest in the Anloga District in the Volta Region. Unlike the Densu Estuary, the catchment basin of Anyanui Creek is less urbanized, however, there is evidence of fertilizer-intensive farming and trading of mangrove wood for livelihood purposes (Mahu et al., 2023). Significant land-cover transformations in the Keta area between 1991 and 2020 are linked to increased cutting of mangroves for fuel wood and fishing traps and clearing the land for agricultural purposes (Duku et al., 2021). The Creek which once recorded a very healthy oyster population is currently witnessing a decrease in the oyster population with remaining populations showing signs of stress including poor growth, and thin and fragile shells. The two cores were collected using a 5 cm diameter × 50 cm length Russian-type corer. Cores were collected in 50 cm sections from overlapping adjacent boreholes with a 10 cm overlap between core sections. On retrieval, sediments were transferred to a PVC pipe and wrapped in aluminum foil ahead of transportation to cold storage. The sediment cores were stored at 4°C until ready for analysis. Each core was sub-sectioned at 1 cm intervals and dried to constant weight at 60°C for all analyses except for trace element scans which were carried out on whole cores. The porosity and dry bulk density were determined at the Department of Environment and Geography Laboratories of the University of York.

Radiocarbon dating of cores and sedimentation rates

Chronologies were developed for each core through the analysis of organic samples (tree bark and charcoal) isolated from selected depths within each core. The organic samples were treated with acid–base–acid (ABA) solution following Brock et al. (2010), to remove soluble carbonates and prevent humic acids from percolating into the sediment sequences. The pre-treated samples were radiocarbon-dated by Acceleration Mass Spectrophotometry (AMS) at the DirectAMS Radiocarbon Dating Facility (Washington, USA). For the Keta core radiocarbon dates were obtained at 50, 100, 150, and 200 cm depths, whereas for the Densu core, dates were obtained at 100 and 150 cm depths. We did not date the 50 cm depth of the Densu core because the prepared samples did not have any charcoal or tree bark material. Age-depth models were constructed using Oxcal 4.4 software (Bronk Ramsey, 1995, 2009) by applying the P-Sequence function, assuming $k_0 = 1$. This method uses information about the order and position of dates within a sequence to constrain posterior age distributions to provide interpolated age range estimates for any given depth (here: 1 cm slices) within a modeled core. Outlier dates were omitted from the model based on the Agreement Index (Bronk Ramsey, 1995), an indicator of the overlap between prior data and the posterior model. Samples were omitted should their agreement index and the overall model be below 60%. Radiocarbon dates were calibrated using the IntCal20 (Reimer et al., 2020) and BombNH2 (Hua et al., 2022) curves for samples dated before and after the year 1950 respectively. Calibrated dates referenced in this study are the mean of the posterior distribution for readability and are reported as BCE/CE.

C, N, C/N ratio, $\delta^{13}C$, and $\delta^{15}N$

Analysis of C, N, δ^{15}N, and δ^{13}C was carried out at the National Environmental Isotope Facility at the British Geological Survey (Nottingham, UK). Oven-dried sediment was analyzed for C and N using a Carlo-Erba CN analyzer, while δ^{15}N and δ^{13}C were measured using an Elementar Vario ISOTOPE cube elemental analyzer (EA) coupled to an Isoprime precisION isotope ratio mass spectrometer (IRMS) with an onboard centrION continuous flow interface system. The EA inlet converts organic materials in solid sample matrices into pure gases via high-temperature combustion. The post-combustion gas mixture is then separated and focused into individual molecular species for quantitative nitrogen and carbon content analysis. It is then passed online to the mass spectrometer to determine the stable isotope composition. The δ^{13}C and δ^{15}N data are reported in delta (δ) notation in per mill (‰) relative to the international reference scales VPDB and AIR, respectively. δ^{13}C data were corrected using a two-point calibration against organic analytical standard B2162 (spirulina, Elemental Microanalysis Ltd.; −18.7‰) and a laboratory working standard (BROC3, −27.6‰). δ^{15}N data were corrected using a multi-point calibration to USGS40 (−4.5‰), USGS41 (+47.6‰), B2162 (+6.1‰), and BROC3 (+1.5‰). The laboratory reference material BROC3 and B2162 have been calibrated for δ^{13}C using IAEA-CH-6 (−10.4‰), USGS54 (−24.4‰), USGS40 (−26.4‰), and B2174 (urea, Elemental Microanalysis Ltd.; −36.5‰), and for δ^{15}N using USGS40 (−4.5‰), IAEA-N-1 (+0.4‰), and IAEA-N-2 (+20.3‰). BROC3 (41.3%C and 4.9%N) was used to calculate the carbon and nitrogen elemental content of samples and C/N is reported as the mass ratio. External precision (1σ) for the within-run standards and sample repeats was ⩽0.1‰ for both δ^{13}C and δ^{15}N.

Trace element analysis

Trace element analysis was carried out at Manor Hall, Department of Archeology, University of York using a high-resolution Handheld Olympus Delta XRF, DPO2000 set to geochemical mode. Each core was scanned at 1 cm intervals until 50 cm, after which scans were made at 10 cm intervals up to the oldest regions. This sampling strategy was adopted due to time constraints that prevented the full length of each core from being analyzed at a high resolution. Instead, we concentrated the high-resolution analyses on the uppermost section of the core, assuming this would contain the most intense periods of anthropogenic activity relevant to the past few centuries. Lower resolution analysis was carried out throughout the rest of the core, allowing us to assess natural variability and characterize conditions before significant levels of disturbance. Both cores were scanned for a wide array of elements; however, only major elements Al, Si, K, Ti, Ca, and Fe, and minor elements Rb, Zn, Sr, Zr, and Mn were detected in the cores. For each core, standards (i.e. silicon) and standard reference material (SRM 2711a) were analyzed between scans. Overall, 18 SRM 2711a were analyzed for both cores. Recoveries ranged from 72.4% for Ca to 130.3% for Zn.

Estimation of geochemical enrichment factors

The enrichment factor evaluates the control of anthropogenic processes on trace metal accumulation in sediments by differentiating between metals originating from anthropogenic sources and those originating from natural sources (Raj and Jayaprakash, 2008). Estimation of trace metal enrichment factor helps to deal with variabilities in trace element concentration associated with natural geochemical factors including grain size effect. It normalizes the measured trace element concentration in the sample with respect to a sample reference element such as Al, Fe, or Ti (Raj and Jayaprakash, 2008).

The element Al was used as the sample reference element in this study since its concentration is derived majorly from natural processes and it is considered one of the most abundant elements in the upper continental crust (Raj and Jayaprakash, 2008). The enrichment factors were estimated from Equation 1.

$$EF = \left[\frac{Ci}{Cie}\right]S \Big/ \left[\frac{Ci}{Cie}\right]RS \qquad (1)$$

Table 1. Radiocarbon and IntCal20 calibrated ages of the Keta and Densu cores retrieved from the Anyanui Creek and Densu Estuary respectively.

Lab code	Core ID	Depth (cm)	Sample type	Fraction modern C		Radiocarbon age		Calibrated ages (Years BP)
				pMC	1 σ error	BP	1 σ error	
D-AMS 046340	KETA	50	Tree bark, charcoal	105.82	0.39	Modern		14 ± 1
D-AMS 046341	KETA	100	Tree bark, charcoal	107.78	0.34	Modern		25 ± 3
D-AMS 046342	KETA	150	Tree bark, charcoal	98.54	0.27	118	22	201 ± 22
D-AMS 046343	KETA	200	Tree bark, charcoal	78.32	0.28	1963	29	1952 ± 29
D-AMS 046345	DENSU	100	Tree bark, charcoal	87.29	0.25	1092	23	1072 ± 23
D-AMS 046346	DENSU	150	Tree bark, charcoal	63.75	0.22	3616	28	3997 ± 28

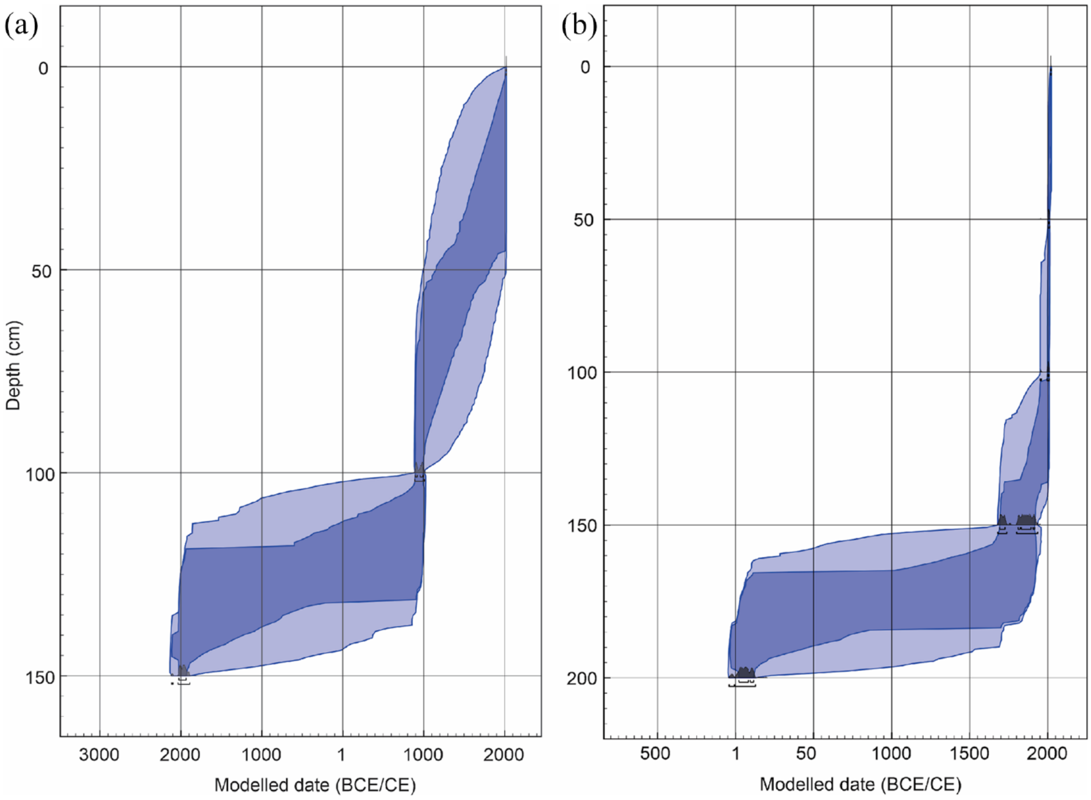

Figure 2. Age-depth curves of Densu (a) and Keta Cores (b) generated in OxCal version 4.4 (Bronk Ramsey, 1995, 2009).

where *Ci* is the element under consideration, the square brackets indicate concentration (usually in mass/mass units, such as mg/kg), *Cie* is a reference element, S is the sample of interest and RS is the reference sample. Upper continental crust (Taylor and McLennan, 1995) was chosen as the reference material for this study. The enrichment factor is interpreted using five categories of enrichment values: $EF < 2$, implying depletion to mineral or natural enrichment; $2 \leq EF < 5$, implying moderate enrichment; $5 \leq EF < 20$, implying significant enrichment; $20 \leq EF < 40$; implying very high enrichment; and $EF > 40$, implying extremely high enrichment in the sediments (Taylor and McLennan, 1995)

Results

Radiocarbon dates, age-depth model, and sedimentation rates

The results of the radiocarbon dating are presented in Table 1 and the modeled chronology for each core is presented in Figure 2. The 150 cm long Densu core was aged to 3997 ± 28 years BP whereas the 200 cm long Keta core was aged to 1952 ± 29 years BP. For the Keta model, an initial run showed poor model agreement (30.2%) caused by low agreement between samples at 200 and 250 cm depths, likely due to the penetration of younger mangrove roots. Removal of these samples greatly enhanced the agreement between priors and posterior data (92.8%); therefore, this was the model that we chose to use in this study. This model indicates that rapid accumulation occurred at approximately 100 cm (1996 CE) to the top of the core, with a mean modeled sedimentation rate of 4 cm/year. Before this, the sedimentation rate was 0.3 cm/year from 1823 CE to 1992 CE and 0.03 cm/year from 62 CE to 1820 CE.

The Densu model showed far better agreement (99.1%). Just like the Keta core, there is a similar rapid increase in sedimentation around 100 cm from 0.02 to 0.1 cm/year. In the Densu core, this shift occurred around the year 960 CE whereas in the KETA core sedimentation rates sharply accelerated in recent times, with a mean date of 1996 CE.

C, N (C/N), $\delta^{13}C$, and $\delta^{15}N$

Downcore variations of C, N, (C/N), $\delta^{13}C$ and $\delta^{15}N$ are shown in Figure 3. Generally, the Densu core shows a decreasing C content upcore (from 2.2% to 0.1%) with values >1% observed between 1384 BCE and 1918 BCE. Like the C, the N content in the Densu core decreases upcore with values ranging from 0.01% to 0.07%.

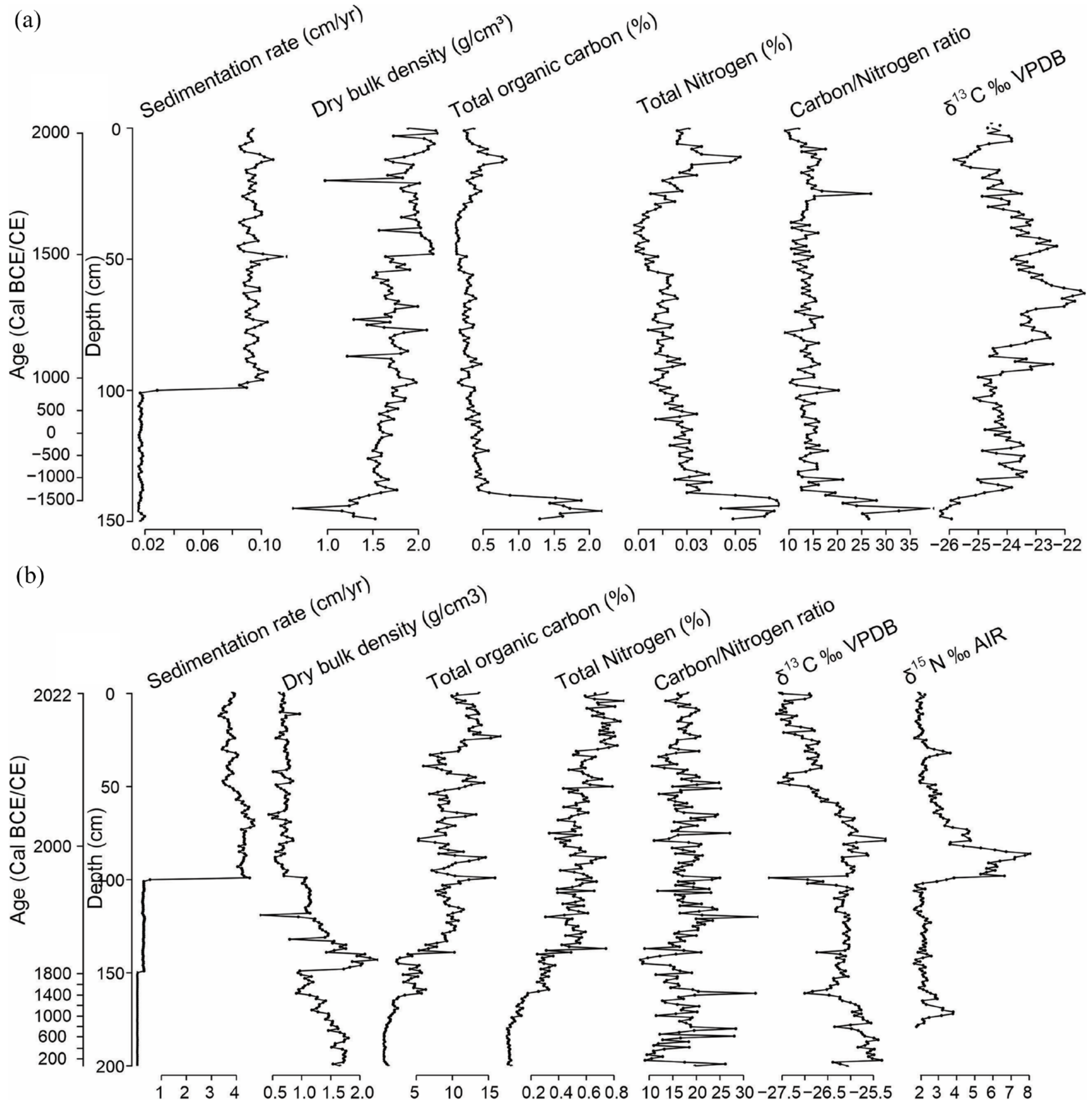

Figure 3. Downcore profiles of sedimentation rates, dry bulk density, C, N, C/N ratio, $\delta^{13}C$ and $\delta^{15}N$ of the Densu (a) and Keta (b) Cores. Negative ages on the y-axis represent BCE years.

Very low values of 0.01% occur between 1678 CE and 1502 CE while high N values (N > 0.06%) occur between 1440 BCE and 1919 BCE. High C/N in the older regions of the core corresponded with low bulk-density values and vice versa. The C/N ratios decreases upcore (from 39 to 9) in the Densu Core. High C/N values (CN > 20) occur between 1440 BCE and 1919 BCE, varied between 19 and 11 between 1384 BCE and 1967 CE, and remained below 10 from 1977 CE to the present. Generally, $\delta^{13}C$ values increase upcore, varying between −26‰ and −23‰. The N content of the Densu core is too low to measure $\delta^{15}N$. Largely, the C and N content of the Keta core increase upcore, varying between 1% and 17%, and 0.03% and 0.9% respectively. High C and N correspond with low bulk density with the later decreasing upcore. Several high peaks implying huge variabilities in both C and N content were observed in the Keta core.

The $\delta^{13}C$ values in the KETA core decrease upcore from −25‰ and −28‰ with low values corresponding to C, N, and C/N peaks. The $\delta^{15}N$ values increase upcore varying between 1.7‰ and 8.1‰ with very high values (i.e. $\delta^{15}N > 4‰$) occurring between 2000 CE and 1996 CE. Due to the very low N content (i.e. N < 0.1) from 758 CE to 62 CE, no $\delta^{15}N$ was measured in this part of the core.

The C, N, $\delta^{13}C$, and $\delta^{15}N$ data in the Keta core are all comparatively higher than in the Densu core, except for $\delta^{13}C$ which increases toward the present and vice versa in the latter. A strong correlation ($R^2 = 0.82$ for Densu and $R^2 = 0.86$ for Keta) exists between N and C in both cores (Figure 4).

Trace element geochemistry

Both major and minor elements show high variability in both the Densu and Keta cores with no distinct trends observed upcore or downcore. In the case of the Densu, major element concentrations varied between 2.7% and 5.8% for Al, 18.4% and 32% for Si, 0.1% and 3.7% for S, 0.1% and 0.5% for K, 0.1% and 4.8% for Ca, 0.2% and 0.4% for Ti, 0.8% and 1.9% for Fe (Figure 5). For the Keta core, major element concentrations vary between 2.3% and 6.2% for Al, 6.9% and 28.2% for Si, 1.3% and 4.7% for S, 0.2% and 0.4% for K, 0.01% and 1.6% for Ca, 0.1% and 0.4% for Ti, 1.2% and 3.0% for Fe (Figure 5). Generally, the levels of all major elements except for Ca are higher in the Keta core relative to the Densu core. The minor element profiles exhibit a high degree of variability down both cores (Figure 6). Minor elements

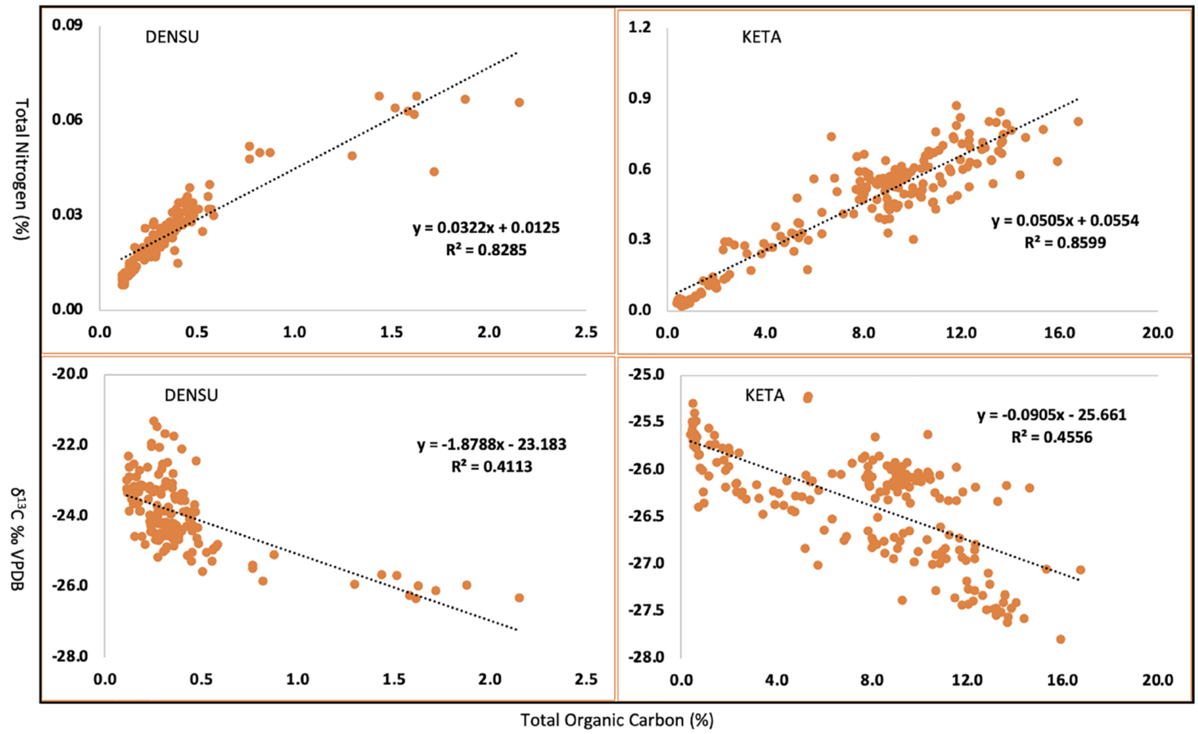

Figure 4. Relationships between total nitrogen (TN), $\delta^{13}C$, and total organic carbon (TOC) in sediment cores from Densu (left) and Keta (right) lagoons.

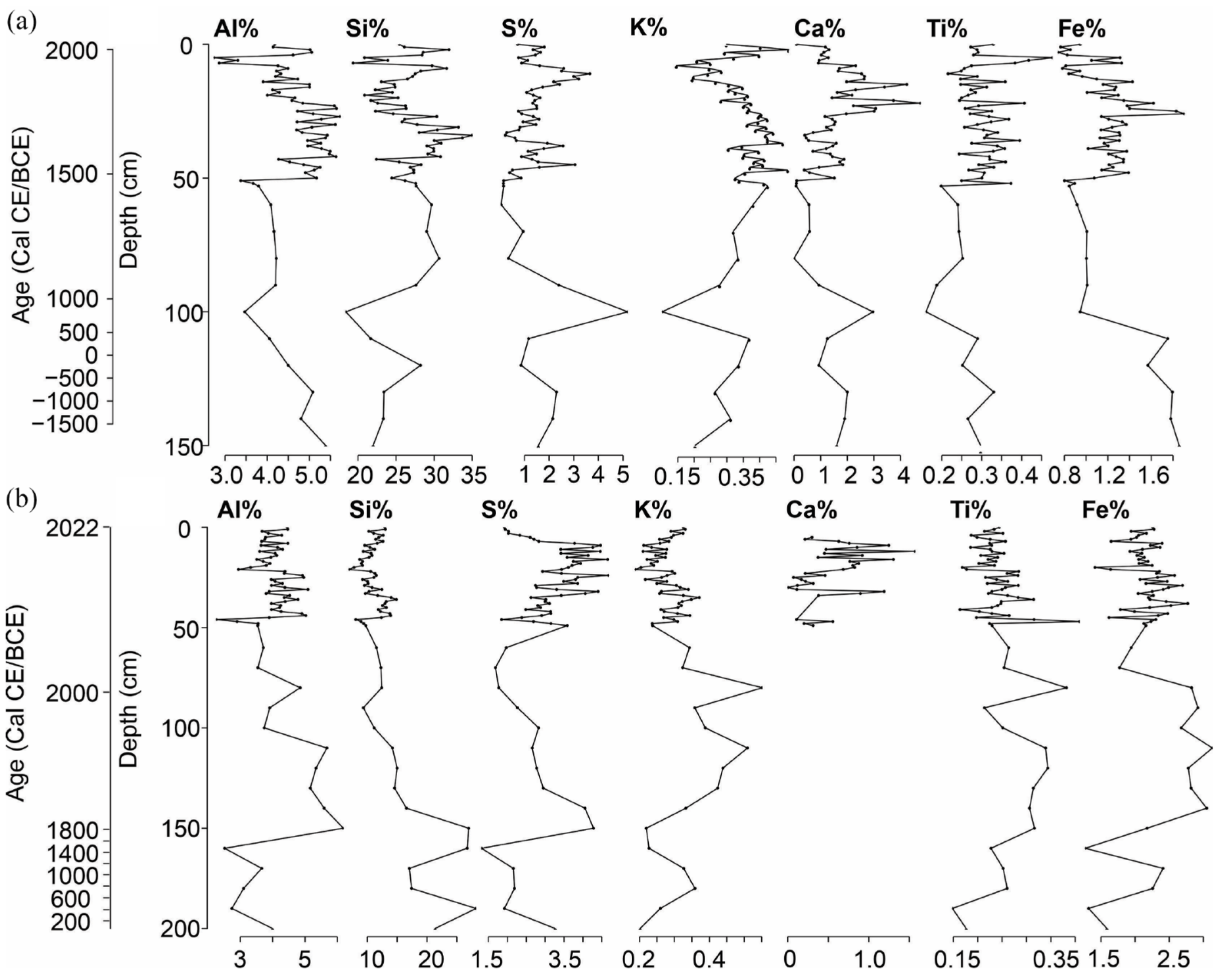

Figure 5. Downcore profiles of Al, Si, S, Ti, and Fe in the Densu (a) and Keta (b) Cores. Negative ages on the *y*-axis represent BCE years.

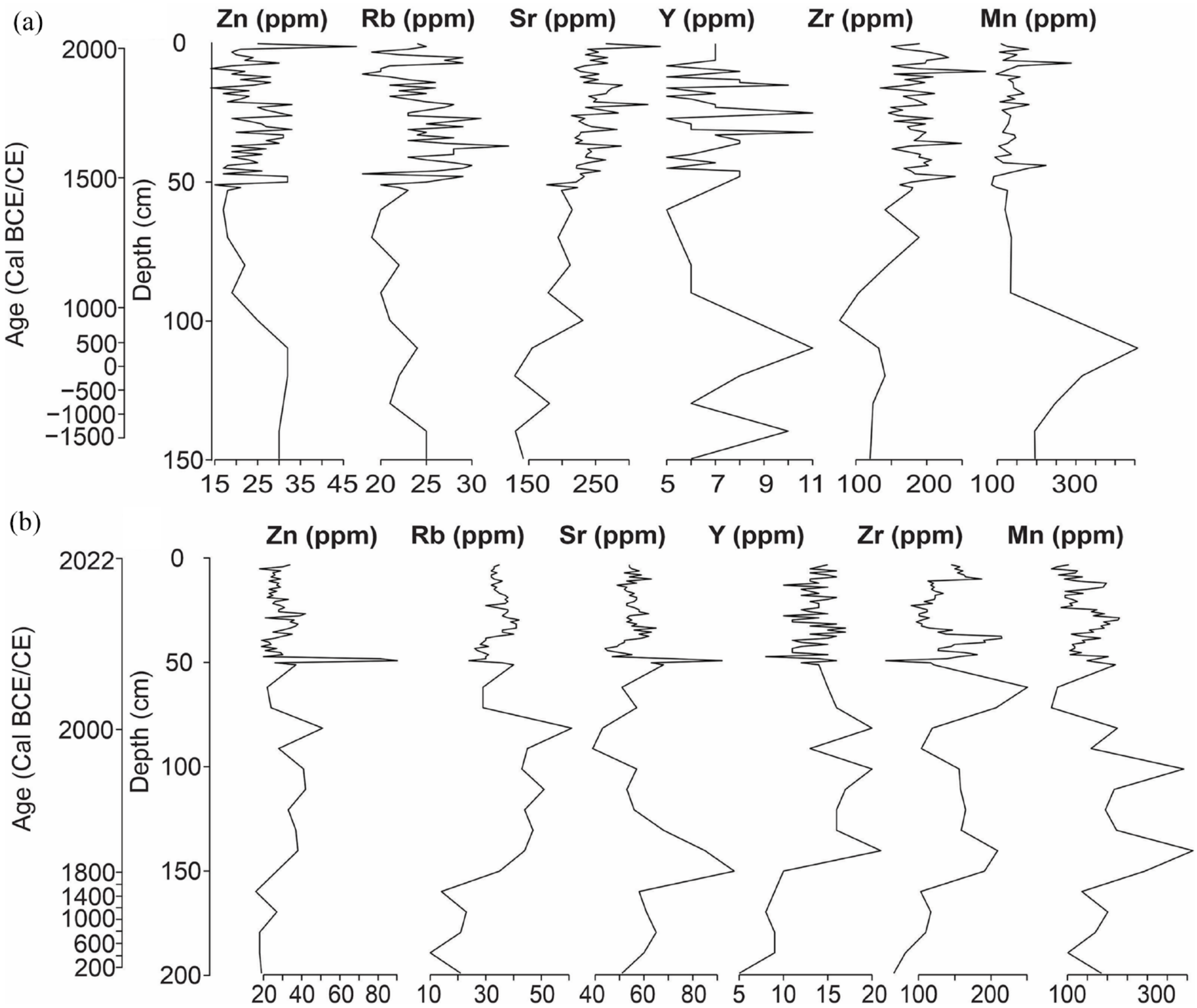

Figure 6. Downcore profiles of Zn, Rb, Sr, Y, Zr, and Mn in the Densu (a) and Keta (b) cores. Negative ages on the *y*-axis represent BCE years.

vary between 14 and 48 ppm for Zn, 18 and 34 ppm for Rb, 129 and 347 ppm for Sr, 77 and 249 ppm for Zr, and 86 and 457 ppm for Mn (Figure 6a). The minor element concentrations in the Keta core vary between 16and 90 ppm for Zn, 10 and 47 ppm for Rb, 47and 67 ppm for Sr, 55 and 215 ppm for Zr, and 74 and 414 ppm for Mn (Figure 6b). The Densu core has comparatively higher Sr relative to the Keta.

Trace element enrichment factors

The variabilities observed in the concentrations of trace elements in Figures 5 and 6 are likely due to geochemical effects such as grain size (Liu et al., 2019), and thus may not necessarily reflect pollution from industrial or mining sources. The level of pollution in the two estuaries with respect to major and minor elements is explained using the estimated enrichment factors. The Densu core shows depletion in S and K, depletion to moderate enrichment in Fe, depletion to significant enrichment in Ti, and significant to extremely high enrichment in S (Figure 7). The Keta core, on the other hand, shows depletion in Ca and K, depletion to moderate enrichment in Si, depletion to significant Ti and Fe, and extremely high enrichment in S (Figure 7). Although no distinct trends in major elements are observed, high enrichment values have been observed in recent times. Though both cores show extremely high enrichment in S, the values are more than 10 times higher in some sections of the Keta relative to the Densu.

For minor elements (Figure 8), the Densu core shows depletion in Rb, and Mn, depletion to moderate enrichment in Zn and Sr, and depletion to significant enrichment in Zr. The Keta core, on the other hand, shows depletion in Rb, Mn, and Sr and depletion to significant enrichment in Zr and Zn. The trends observed in the profiles of enrichment factors for minor elements are not different from what was observed for the major elements in both cores.

Discussion

Radiocarbon dates and sedimentation rates

Obtaining reliable chronologies from mangrove sediments is challenging, due to the complexity of mangrove carbon cycling (Sefton et al., 2021) and the dynamic sedimentary environment (Peros et al., 2015). The use of ligneous remains and charcoal as dating material may mean that the dates reported in this study may have been affected by the "old wood effect," whereby woody remains and charcoal can be much older than the sediments in which they are deposited within (Schiffer, 1986). It is difficult to assess the accuracy of these age-depth models due to these uncertainties, in addition to the limited number of dates available in the study. Despite these limitations, the models generated show a reasonable agreement with the data. As well as showing agreement with stratigraphic shifts seen in the profiles of C and N in both cores, these dates provide an interpretative chronological framework for the chemical analysis.

The sedimentation rate in estuarine environments is partly controlled by the sediment supply, which depends on factors such

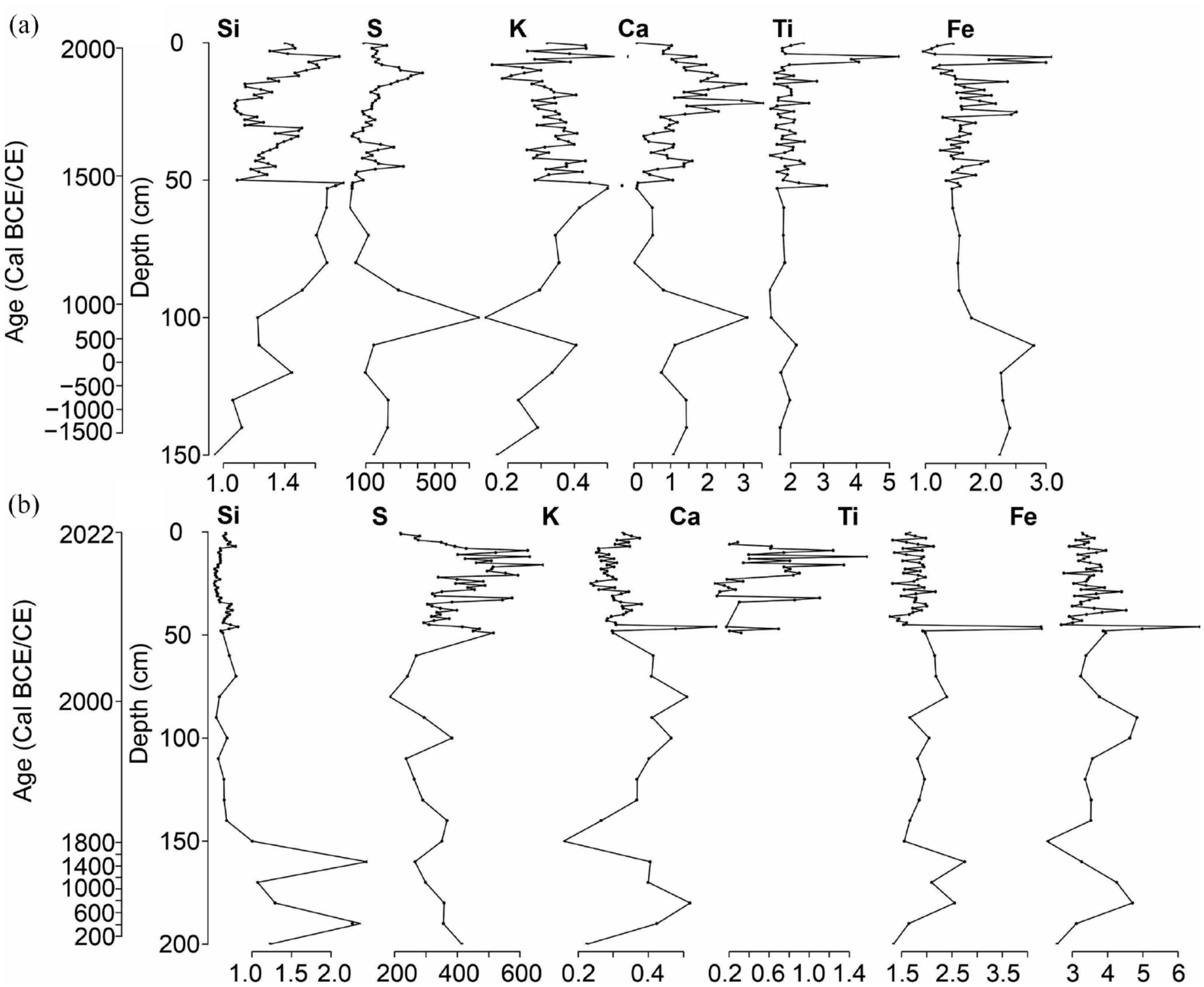

Figure 7. Profiles of Enrichment Factors for Si, S, K, Ca, Ti, Fe, and La for the Densu (a) and Keta (b) Cores.

as climate, the transformation of a river, and its catchment, as well as other processes occurring in the sea (Armitage et al., 2011). While natural events such as floods can significantly affect sedimentation rates, most of the factors are linked to human activities like reclamation, urbanization, industrialization, and deforestation (Godoy et al., 2012; Sanders et al., 2016). Although sedimentation rates were far slower in the Densu core compared with those obtained at Keta, coincidentally, both cores showed a rapid increase in sedimentation rate observed at around 100 cm depth. At first glance, the coincidental alteration in sedimentation rate at the 100 cm mark may be interpreted as stemming from comparable natural or anthropogenic factors influencing the shift in sedimentation regime in both estuaries. However, it is important to note that the two depths represented different ages in both cores. In the case of the Densu core, the rapid shift in sedimentation rate at 100 cm overlaps with the year 960 CE whereas in the KETA the shift at 100 cm is more recent occurring around 1996 CE. This suggests that different factors could be driving the sediment inflow and variabilities within the two systems. For the Keta core, we attribute this recent and significant change in sedimentation rate to human-induced alterations in land use and land cover dynamics within the Anloga-Anyanui area, notably the extensive harvesting and trade of mangroves for fuel wood (Aheto et al., 2016; Sekey et al., 2023) and clearing of land for farming purposes (Mahu et al., 2023). During the period from 1991 to 2020, a total of 37.6% of mangrove/dense vegetation cover, equivalent to 200.2 km², was lost in the Keta-Anyanui area (Duku et al., 2021). This unusual harvesting of mangroves and the resultant loss in forest coverage has created several kilometers of bare earth within the Creek's catchment, consequently accelerating the influx of sediment into the Creek. In the Densu core, the observed periodic shift in sedimentation rate coincides with a sharp decrease in $\delta^{13}C$, spikes in $\delta^{15}N$, and a high C/N ratio at 960 CE, suggesting historical catchment changes arising from either anthropogenically driven land-use change or climatic variations such as extended periods of drought accompanied by flood events. We argue that the latter is a more probable cause of the sedimentation shift in the Densu because population growth and heavy land-use transformation are quite recent dating back to the late 90s. On the other hand, significant expansion in the built environment, mainly housing and gray infrastructure during the mid to late 90s within the watershed of Densu coupled with damming of the Densu River is likely the cause of low sedimentation rates observed in recent times in the Densu.

While oysters occur on sediment beds and have the potential to naturally filter sediments, heavy sediment loads may be detrimental to their growth and survival; in the case of the Anyanui Creek, this rapidly increasing sedimentation rate is likely to pose challenges to oyster feeding, growth, and survival. Several studies have established that heavy sediment loads in estuaries impact oyster larval settlement (Poirier et al., 2021), and impair respiration and feeding rates in juvenile and adult oysters (Loosanoff, 1962; Loosanoff and Tommers, 1948; Wilber and Clarke, 2010). Although adult oysters can discern between inert and organic particulates (Gonda-King et al., 2010), at higher levels of siltation and sediment accumulation, they generally reduce valve opening and filtration time, which negatively affects their growth rates (Gonda-King et al., 2010). Sedimentation impacts on bivalves are

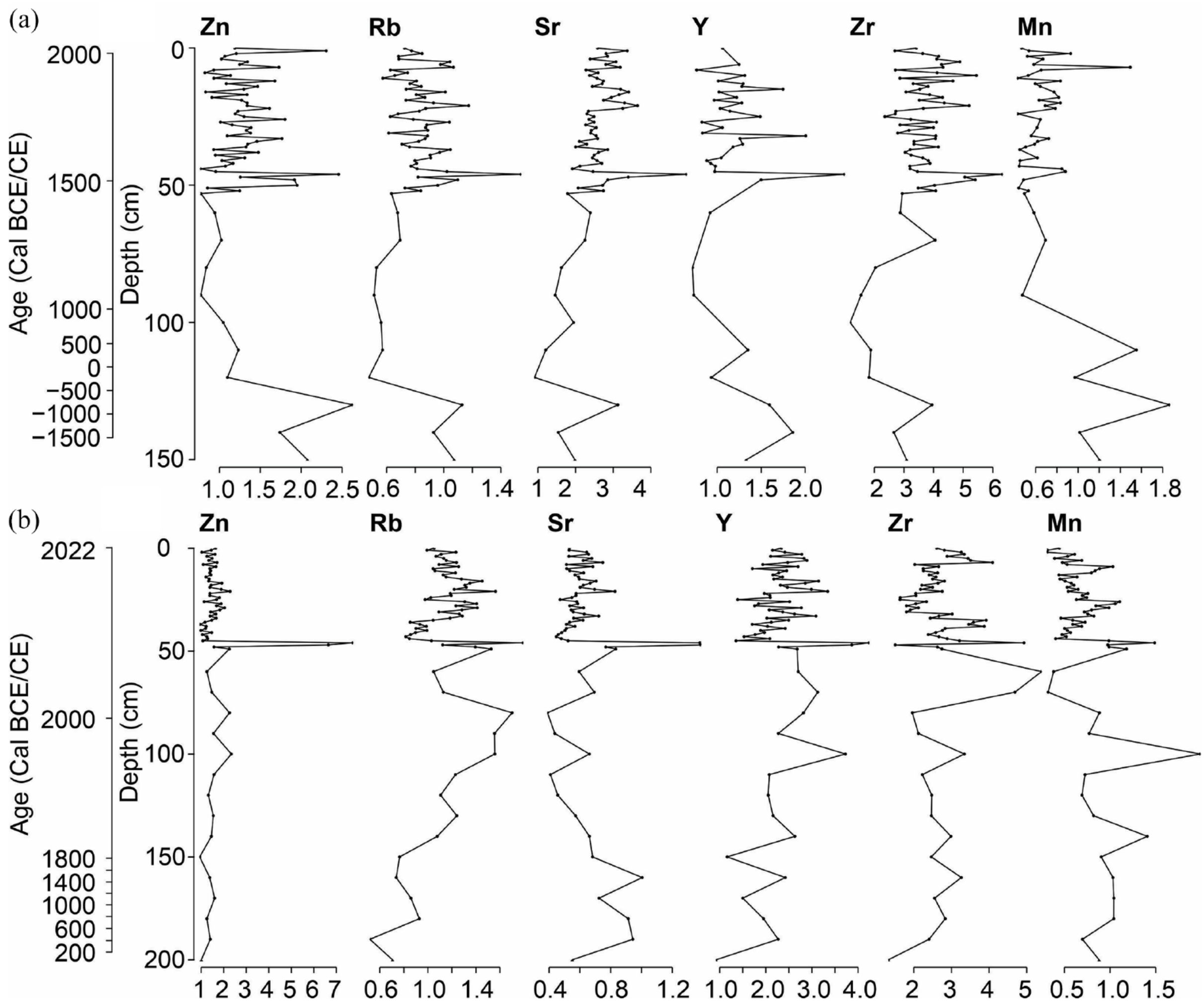

Figure 8. Profiles of enrichment factors for Zn Rb, Sr, Y, Zr, and Mn in the Densu (a) and Keta (b). Negative ages on the y-axis represent BCE years.

of broader concern for ecosystem health, wild fisheries, and the associated livelihoods. Unpublished data on historical growth rate of oysters in the Anyanui Creek and Densu Estuary show very slow growth rates in the former compared to the latter with improved growth rates in the latter observed in recent times.

C, N (C/N), δ^{13}C, and δ^{15}N

Enhanced C in aquatic ecosystems can be both beneficial and detrimental to benthic organisms (Pearson, 1978). The extremely high levels of C in the Keta core compared to the Densu core align with the high sedimentation rate in the Anyanui Creek which is attributed to intense vegetation cover removal, turning forested lands in the catchment basin bare, particularly in recent years. The C content in aquatic ecosystems is influenced by initial biomass production and subsequent degradation, thus integrating the different processes of organic matter source, delivery routes, depositional, and preservation (Meyers, 2003). High sedimentation rates and increasing grain size inferred from the dry bulk density measurement imply short transport time for the sinking particles, and subsequently, low exposure to water column oxidation resulting in higher preservation of C in the Keta core. Thus, the C content in the sediment could represent a bulk value of organic matter that escaped remineralization during sedimentation and subsequent burial.

The C/N ratio is important in the discrimination of organic matter sources in aquatic ecosystems. Typically, algae have molar C/N values that are commonly between 4 and 10, whereas vascular land plants, which are protein-poor and cellulose-rich, create organic matter that usually has C/N ratios of 20 and greater (Meyers, 1994). The higher C/N ratio and δ^{13}C values in the Keta core, particularly in recent times, depict the dominance of organic matter originating from higher terrestrial plants. The marine algae organic matter dominance observed in the mid-1800s in the Keta core suggests a substantial change in land cover during this period which could have reduced terrestrial and fluvial input, promoting in-estuary tidal production of algal organic matter. The C/N and δ^{13}C of the Densu core on the other, show a distinct progression from higher vascular plant dominance (high C/N ratios, lower δ^{13}C values) of organic matter from the oldest region of the core to marine algae dominance of organic matter (low C/N ratios, higher δ^{13}C values) from 1977 CE to present day. An explanation for this change could be a reduction in land-based or riverine organic matter flux into the Densu estuary through time arising from catchment transformation including deforestation to wetland vegetation degradation to the establishment of a well-built environment (Antwi-Agyakwa, 2014; Frank et al., 2019). The period coincides with the construction of the Weija Dam in the year 1978 on the Densu River (Kuma and Ashley, 2008). It is obvious from this study how the damming of the Densu River has changed the organic matter dynamics and geochemical outlook of the Densu estuary. The estuary is now totally opened to the adjacent sea with limited freshwater input only when there is dam spillage or precipitation. This gives it near or typical seawater salinities (>25 PSU) during most times of the year. The Keta core on the other hand portrays a system dominated by freshwater influx with little seawater influence with a measured salinity ranging between 5 and 12 PSU. Salinity is among the most important factors affecting the growth and survival of oysters (Davis, 1958; Nell and Holliday, 1988; Tan and Wong, 1996; Wang and Li, 2018), with changes in salinity regarded as one of the most significant environmental stressors for oysters. In a previous study, a very high vulnerability index of 12 estimated for the West African Mangrove oyster *C. tulipa* places it among marine organisms that are highly vulnerable to climate change and climate variability (Mahu et al., 2022). Salinity fluctuations driven by variabilities in precipitation and sea level rise is among the most important exposure factors driving this very high vulnerability score. Though adapted to live in a wide range of salinities from 4 to 50 ppt (Mahu et al., 2022), higher salinities have yielded high feeding, growth, and breeding success in the West African mangrove oysters (Sutton et al., 2012; Yankson, 1990). Hence in the case of the Keta-Anyanui Creek, our data on reducing salinity in the Creek is well corroborated by the declining growth rate and large mortalities we are observing in the Creek.

The composition of $\delta^{15}N$ in aquatic sediment can be linked to various factors (in a similar way to $\delta^{13}C$) including nitrogen source, nutrient cycling processes, organic matter input, redox conditions, changing rates of sedimentation for marine and terrestrial input, and anthropogenic processes (Sebilo et al., 2019; Sweeney and Kaplan, 1980). Terrestrial nitrogen compounds discharged as sewage effluent can be differentiated by $\delta^{15}N$ from non-sewage-related nitrogen compounds. Redox conditions in sediments, particularly, oxygen availability can influence the $\delta^{15}N$, with aerobic conditions favoring nitrification, which can result in $\delta^{15}N$ depletion and anaerobic conditions promoting denitrification, leading to $\delta^{15}N$ enrichment (Ke et al., 2019). Also, sedimentation rates can affect the preservation of organic matter in sediments with higher sedimentation rates implying faster burial of organic material. This preservation of organic matter decreases exposure to oxygen and microbial degradation, maintaining the original $\delta^{15}N$ signature of the organic matter. While it is difficult to ascertain the exact control on $\delta^{15}N$ in both cores, the contrasting sedimentation rates in the two cores are likely to play a role in higher $\delta^{15}N$ enrichment in the Keta core and lower $\delta^{15}N$in the Densu core. The high $\delta^{15}N$ values from the change in sedimentation to the top of the Keta core imply faster burial of organic matter and therefore the high $\delta^{15}N$ values. Again, from the $\delta^{13}C$ profiles, the Densu core has higher $\delta^{13}C$ compared to the Keta Core, suggesting more algae-generated organic matter in the former and terrestrial organic matter dominance in the latter. Considering that generally, marine plants tend to have lower $\delta^{15}N$ compared to terrestrial plants (Hoffman et al., 2008), the variabilities in $\delta^{15}N$ in both cores provide further evidence of dominant marine-dominated processes in the Densu Estuary and terrestrial-dominated processes in the Anyanui Creek.

Trace element geochemistry and enrichment

Sulfur (S) deposition in sediments is higher in eutrophic than in oligotrophic sediments due to higher rates of S reduction, enhanced sedimentation of organic S, and less reoxidation (Holmer and Storkholm, 2001). The extremely high enrichment of S and Fe in both cores suggest potential ongoing reduction processes at various scales at the bottom of both the Densu estuary and the Anyanui Creek. These reduction processes could have created chemical boundaries leading to the enrichment of other trace elements and $\delta^{15}N$ (described above) in the cores. A study conducted on surface sediments for the Densu Estuary showed high and low enrichments of Fe and Mn respectively in the sediments (Akita et al., 2020). The intensity of the reduction processes in the bottom could trigger other chemical processes such as ocean acidification and hypoxia, which has the potential to induce larvae mortality and retard growth in juveniles and adult oysters (Jeppesen et al., 2018; Lemasson et al., 2017; Stevick et al., 2021). In unpublished data, we consistently find very low dissolved oxygen and anoxic conditions in some parts of the Keta-Anyanui Creek. These low oxygen levels, coupled with high sedimentation rate, high nutrient and organic matter content, and low salinity in the Keta-Anyanui Creek present the oysters with coping and adaptation struggles contributing to the poor growth conditions and increasing mortalities witnessed in the Creek. Also, oysters and bivalves in general have the potential to bioaccumulate trace elements (Mok et al., 2015; Rodrigues et al., 2022; Zhu et al., 2020), implying that oysters in both estuaries may be incorporating more than acceptable levels of trace elements into their tissues. Recent studies on heavy metal accumulation in oyster tissues from some selected estuaries in Ghana including the Densu, reported high levels of heavy metals in the tissues of the oyster (Owusu-Prempeh et al., 2022). This potential of oysters to bioconcentrate trace metals has dire implications for their ecological functioning and ecosystem processes as well as for human health.

Conclusions

Oyster fisheries support the livelihoods of vulnerable artisanal coastal communities along the West African Coast. In addition, they render a suite of ecosystem services to coastal environments in the region. However, their landings and numbers have declined significantly in the past century. The study documents evidence of changing geochemical conditions in two oyster environments, Densu Estuary and keta-Anyanui Creek in Ghana through high-resolution studies of two sediment cores, highlighting likely impacts to the oyster fishery.

Rapid shifts in sedimentation rates have occurred in both ecosystems through time, however, in the keta-Anyanui Creek, the change in sedimentation rate was more pronounced, and occurred very recently starting from c.1996 CE to the present. In the case of the Densu estuary, the change in sedimentation rate was comparatively little slower and occurred late in the core at c.960 CE. The shift in sedimentation of the Anyanui Creek coincides with periods of intense land cover change that is, mangrove degradation and vegetation clearing in the Anloga-Anyanui catchment.

High organic matter accumulation is observed in the Keta-Anyanui Creek relative to the Densu estuary core with C levels in the former about nine times that observed in the latter. The trend observed in C levels agrees with the sedimentation rate in the Anyanui Creek with C levels increasing up the core. On the contrary, the Densu core shows an increasing C content downcore with high C values corresponding to the oldest parts of the core. The trends in N content are like those observed in C for both cores respectively with C and N showing strong correlations.

The C/N ratio and $\delta^{13}C$ values of the Keta core suggest organic matter dominated mainly by wetland vegetation with little algae. The C/N ratio and $\delta^{13}C$ values of the Densu core show a progression from higher vascular plant dominance of organic matter from the oldest region of the core, followed by mangrove dominance by c.1977 CE, and from then on depicting increasing marine algae to present day. The period of transitioning from mangrove dominance to marine algae dominance coincide with the daming of the Densu River in 1978. This observation in the Densu estuary clearly demonstrates a catchment basin that has witnessed various degrees of transformation possibly starting from massive removal of forest cover to wetland vegetation degradation and the establishment of a well-built environment in present-day.

Extremely high enrichment in S and moderate to significant enrichment of Fe were observed in both the Keta and Densu cores' though higher in Keta. These elevated levels in metals suggest possible ongoing reduction processes at various scales at the bottom of both the Densu estuary and the Keta-Anyanui Creek, particularly in the latter.

The changes in sediment geochemistry in both cores reflect ongoing changes in the chemical and physical signatures and consequently the health of these ecosystems at a timescale that has not been documented previously. Broadly, these changes will impact the biodiversity and other services such as fisheries production provided by the two ecosystems. With respect to the oyster fisheries, we show from these geochemical data how this globally threatened fishery is being impacted by changing local environmental conditions. With the poorest conditions that is, very high sedimentation rate, high organic matter accumulation, high $\delta^{15}N$, high S, and low oxygen levels and salinity documented in the Keta-Anyanui Creek, we conclude that oysters in this environment face serious coping and adaptation challenges. These challenges are evident in the poor growth rate and population health seen in the oyster fishery in the Keta-Anyanui Creek during the past five decades. The changes observed in the health of both environments are largely driven by various transformations in the catchment basin of the two ecosystems, which in the case of Keta-Anyanui, comprise the harvesting and trading of mangroves as well as clearing of the land for agriculture purposes. Such transformations in the catchment will not only impact the oyster fisheries, rather the impacts will extend to the wider inshore biodiversity and fisheries with wide ramifications to livelihoods and the functioning of this important wetland, RAMSAR, and Key Biodiversity Areas. We recommend management actions that prioritize catchment basin protection, ecosystem restoration, and alternative livelihoods devoid of mangrove trading for coastal communities. Future research should focus on addressing questions on the response of oysters to specific geochemical parameters by looking at their direct or indirect impacts on the health of oyster environments. Studies should also focus on devising coping and adaptation strategies that promote oyster population growth to support livelihoods and enhance ecosystem services.

Acknowledgements

The authors are grateful to laboratory technicians at the Department of Marine and Fisheries Sciences at the University of Ghana, the British Geological Survey, and the University of York for their immense support during the laboratory work, particularly Gareth Perry for providing his assistance and expertise toward the uXRF analyses in this study.

Author contribution

Edem Mahu: Conceptualized, supervised, and received funding for the study as well as participated in field sampling and data analysis, and wrote the main manuscript.
Melanie J Leng: Assisted with stable isotope and elemental analysis and review of the main manuscript.
Luke Andrews: Assisted with XRF analysis, modeling of radiocarbon dates, data visualization, and review of the manuscript.
Apichaya Englong: Assisted with sample preparation and review of the manuscript.
Robert Marchant: Assisted with study design, supervision of study, and writing of the main manuscript. All authors approved the final manuscript to be submitted.

Funding

The author(s) disclosed receipt of the following financial support for the research, authorship, and/or publication of this article: This research was funded by The Royal Society through the Future Leaders African Independent Research (FLAIR) Fellowship program through grant number FLR\R1\201385.

Ethical Statement

This article does not contain any studies with human or animal participants.

ORCID iD

Edem Mahu https://orcid.org/0000-0002-0212-8150

References

Aheto DW, Kankam S, Okyere I et al. (2016) Community-based mangrove forest management: Implications for local livelihoods and coastal resource conservation along the Volta estuary catchment area of Ghana. *Ocean & Coastal Management* 127: 43–54.

Akita LG, Laudien J and Nyarko E (2020) Geochemical contamination in the Densu estuary, Gulf of Guinea, Ghana. *Environmental Science and Pollution Research* 27: 42530–42555.

Andersson RA, Meyers P, Hornibrook E et al. (2012) Elemental and isotopic carbon and nitrogen records of organic matter accumulation in a Holocene permafrost peat sequence in the East European Russian Arctic. *Journal of Quaternary Science* 27(6): 545–552.

Antwi-Agyakwa KT (2014) *Assessing the effect of land use land cover change on Weija catchment*. MSc Thesis, Kwame Nkrumah University of Science and Technology, Ghana.

Armitage JJ, Duller RA, Whittaker AC et al. (2011) Transformation of tectonic and climatic signals from source to sedimentary archive. *Nature Geoscience* 4: 231–235.

Baker S and Mann R (1994) Description of metamorphic phases in the oyster Crassostrea virginica and effects of hypoxia on metamorphosis. *Marine Ecology Progress Series* 104: 91–99.

Beck MW, Brumbaugh RD, Airoldi L et al. (2011) Oyster reefs at risk and recommendations for conservation, restoration, and management. *Bioscience* 61(2): 107–116.

Bernoux M, Cerri CC, Neill C et al. (1998) The use of stable carbon isotopes for estimating soil organic matter turnover rates. *Geoderma* 82(1-3): 43–58.

Brock F, Higham T, Ditchfield P et al. (2010) Current pretreatment methods for AMS radiocarbon dating at the Oxford Radiocarbon Accelerator Unit (ORAU). *Radiocarbon* 52(1): 103–112.

Bronk Ramsey C (1995) Radiocarbon calibration and analysis of stratigraphy: The OxCal program. *Radiocarbon* 37(2): 425–430.

Bronk Ramsey C (2009) Bayesian analysis of radiocarbon dates. *Radiocarbon* 51(1): 337–360.

Capelle DW, Kuzyk ZZA, Papakyriakou T et al. (2020) Effect of terrestrial organic matter on ocean acidification and CO2 flux in an Arctic shelf sea. *Progress in Oceanography* 185: 102319.

David E, Tanguy A, Pichavant K et al. (2005) Response of the Pacific oyster Crassostrea gigas to hypoxia exposure under experimental conditions. *FEBS Journal* 272(21): 5635–5652.

Davis HC (1958) Survival and growth of clam and oyster larvae at different salinities. *Biology Bulletin* 114(3): 296–307.

Duku E, Mattah PAD and Angnuureng DB (2021) Assessment of land use/land cover change and morphometric parameters in the keta Lagoon Complex Ramsar site, Ghana. *Water* 13(18): 2537.

Frank OA, Kwaku AA, Emmanuel O et al. (2019) Trends in land use/land cover changes in the Densu River basin and its impact on the Weija reservoirs and the Densu delta (Sakumo I lagoon) in Ghana. *Journal of Geography and Regional Planning* 12(4): 76–89.

Gazeau F, Gattuso J-P, Greaves M et al. (2011) Effect of carbonate chemistry alteration on the early embryonic development of the Pacific oyster (Crassostrea gigas). *Plos One* 6(8): e23010.

Godoy JM, Oliveira AV, Almeida AC et al. (2012) Guanabara Bay sedimentation rates based on ^{210}Pb dating: Reviewing the existing data and adding new data. *Journal of the Brazilian Chemical Society* 23: 1265–1273.

Gonda-King LM, Keppel AG, Kuschner MA et al. (2010) *The Relation of Sedimentation to Growth Rate in the Eastern Oyster (Crassostrea virginica)*. St. Mary's City: St. Mary's College of Maryland.

Hoffman JC, Bronk DA and Olney JE (2008) Organic matter sources supporting lower food web production in the tidal freshwater portion of the York River estuary, Virginia. *Estuaries and Coasts* 31: 898–911.

Holmer M and Storkholm P (2001) Sulphate reduction and sulphur cycling in lake sediments: A review. *Freshwater Biology* 46(4): 431–451.

Hopkinson CS, Buffam I, Hobbie J et al. (1998) Terrestrial inputs of organic matter to coastal ecosystems: An intercomparison of chemical characteristics and bioavailability. *Biogeochemistry* 43: 211–234.

Hua Q, Turnbull JC, Santos GM et al. (2022) Atmospheric radiocarbon for the period 1950–2019. *Radiocarbon* 64(4): 723–745.

Jeppesen R, Rodriguez M, Rinde J et al. (2018) Effects of hypoxia on fish survival and oyster growth in a highly eutrophic estuary. *Estuaries and Coasts* 41: 89–98.

Kennish MJ (2002) Environmental threats and environmental future of estuaries. *Environmental Conservation* 29(1): 78–107.

Ke Z, Tan Y, Huang L et al. (2019) Significantly depleted 15N in suspended particulate organic matter indicating a strong influence of sewage loading in Daya Bay, China. *Science of the Total Environment* 650: 759–768.

Kuma J and Ashley D (2008) Runoff estimates into the Weija reservoir and its implications for water supply to the Accra area, Ghana. *Journal of Urban and Environmental Engineering* 2(2): 33–40.

Lemasson AJ, Fletcher S, Hall-Spencer JM et al. (2017) Linking the biological impacts of ocean acidification on oysters to changes in ecosystem services: A review. *Journal of Experimental Marine Biology and Ecology* 492: 49–62.

Leng MJ and Lewis JP (2017) C/N ratios and carbon isotope composition of organic matter in estuarine environments. In: Weckström K, Saunders K, Gell P et al. (eds) *Applications of Paleoenvironmental Techniques in Estuarine Studies*. Dordrecht: Springer Netherlands, pp.213–237.

Liu D, Bertrand S and Weltje GJ (2019) An empirical method to predict sediment grain size from inorganic geochemical measurements. *Geochemistry Geophysics Geosystems* 20(7): 3690–3704.

Loosanoff V (1962) Effects of turbidity on some larval and adult bivalves. In: *Proceedings of the Gulf and Caribbean fisheries institute*, 14, 80–95. Institute of Marine Science, University of Miami.

Loosanoff VL and Tommers FD (1948) Effect of suspended silt and other substances on rate of feeding of oysters. *Science* 107(2768): 69–70.

Mahu E, Danso P, Edusei MO et al. (2023) Impact of agricultural practices on ecosystem health of lagoons: A case study of the keta Lagoon Complex in Ghana, West Africa. *Environmental Monitoring and Assessment* 195(5): 622–715.

Mahu E, Sanko S, Kamara A et al. (2022) Climate resilience and adaptation in West African oyster fisheries: An expert-based assessment of the vulnerability of the oyster crassostrea tulipa to climate change. *Fishes* 7(4): 205.

Medina E and Francisco M (1997) Osmolality and δ13C of leaf tissues of mangrove species from environments of contrasting rainfall and salinity. *Estuarine Coastal and Shelf Science* 45(3): 337–344.

Meyers PA (1994) Preservation of elemental and isotopic source identification of sedimentary organic matter. *Chemical Geology* 114(3-4): 289–302.

Meyers PA (2003) Applications of organic geochemistry to paleolimnological reconstructions: A summary of examples from the Laurentian Great Lakes. *Organic Geochemistry* 34(2): 261–289.

Mok JS, Yoo HD, Kim PH et al. (2015) Bioaccumulation of heavy metals in oysters from the southern coast of Korea: Assessment of potential risk to human health. *Bulletin of Environmental Contamination and Toxicology* 94: 749–755.

Montagna P, Palmer TA and Pollack JB (2012) *Hydrological Changes and Estuarine Dynamics*. New York, NY: Springer Science & Business Media.

Nell JA and Holliday JE (1988) Effects of salinity on the growth and survival of Sydney rock oyster (Saccostrea commercialis) and Pacific oyster (Crassostrea gigas) larvae and spat. *Aquaculture* 68(1): 39–44.

North EW, King DM, Xu J et al. (2010) Linking optimization and ecological models in a decision support tool for oyster restoration and management. *Ecological Applications* 20(3): 851–866.

Owusu-Prempeh N, Awuah KO, Abebrese IK et al. (2022) Analysis of the status and ecological risks of heavy metals contamination in artisanal and small-scale gold mine-spoils at the Atewa Forest Landscape, Ghana. *Scientific African* 16: e01235.

Patterson HK, Boettcher A and Carmichael RH (2014) Biomarkers of dissolved oxygen stress in oysters: A tool for restoration and management efforts. *Plos One* 9(8): e104440.

Pearson T (1978) Macrobenthic succession in relation to organic enrichment and pollution of the marine environment. *Oceanography and Marine Biology: An Annual Review* 16: 229–311.

Perdue EM and Koprivnjak J-F (2007) Using the C/N ratio to estimate terrigenous inputs of organic matter to aquatic environments. *Estuarine Coastal and Shelf Science* 73(1-2): 65–72.

Peros M, Gregory B, Matos F et al. (2015) Late-Holocene record of lagoon evolution, climate change, and hurricane activity from southeastern Cuba. *Holocene* 25(9): 1483–1497.

Poirier LA, Clements JC, Coffin MRS et al. (2021) Siltation negatively affects settlement and gaping behaviour in eastern oysters. *Marine Environmental Research* 170: 105432.

Raj SM and Jayaprakash M (2008) Distribution and enrichment of trace metals in marine sediments of Bay of Bengal, off Ennore, south-east coast of India. *Environmental Geology* 56: 207–217.

Reimer PJ, Austin WEN, Bard E et al. (2020) The IntCal20 Northern Hemisphere radiocarbon age calibration curve (0–55 cal kBP). *Radiocarbon* 62(4): 725–757.

Rodrigues LJ, Blemker SR, Frangos SC et al. (2022) Bioaccumulation of trace metals in two oyster species from southwest Puerto Rico. *Marine Pollution Bulletin* 178: 113581.

Sanders CJ, Santos IR, Maher DT et al. (2016) Examining (239+240)Pu, (210)Pb and historical events to determine carbon, nitrogen and phosphorus burial in mangrove sediments of Moreton Bay, Australia. *Journal of Environmental Radioactivity* 151 Pt 3(Part 3): 623–629.

Schiffer MB (1986) Radiocarbon dating and the "old wood" problem: The case of the Hohokam chronology. *Journal of Archaeological Science* 13(1): 13–30.

Sebilo M, Aloisi G, Mayer B et al. (2019) Controls on the isotopic composition of nitrite (δ15N and δ18O) during denitrification in freshwater sediments. *Scientific Reports* 9(1): 19206.

Sefton J, Woodroffe S and Ascough P (2021) Radiocarbon dating of mangrove sediments. In: *Dynamic Sedimentary Environments of Mangrove Coasts* (pp.199–215). Elsevier.

Sekey W, Obirikorang KA, Boadu KB et al. (2023) Mangrove plantation and fuelwood supply chain dynamics in the keta Lagoon Complex Ramsar site, Ghana. *Wetlands Ecology and Management* 31(1): 143–157.

Stevick RJ, Post AF and Gómez-Chiarri M (2021) Functional plasticity in oyster gut microbiomes along a eutrophication gradient in an urbanized estuary. *Animal Microbiome* 3(1): 17.

Sutton A, Yankson K and Wubah D (2012) The effect of salinity on particle filtration rates of the west African mangrove oyster. *Journal of Young Investigators* 24(4): 55–59.

Sweeney RE and Kaplan IR (1980) Natural abundances of 15N as a source indicator for near-shore marine sedimentary and dissolved nitrogen. *Marine Chemistry* 9(2): 81–94.

Tan S-H and Wong T-M (1996) Effect of salinity on hatching, larval growth, survival and settling in the tropical oyster Crassostrea belcheri (Sowerby). *Aquaculture* 145(1-4): 129–139.

Taylor SR and McLennan SM (1995) The geochemical evolution of the continental crust. *Reviews of Geophysics* 33(2): 241–265.

Wallace RB, Baumann H, Grear JS et al. (2014) Coastal ocean acidification: The other eutrophication problem. *Estuarine Coastal and Shelf Science* 148: 1–13.

Wang T and Li Q (2018) Effects of salinity and temperature on growth and survival of juvenile Iwagaki oyster Crassostrea nippona. *Journal of Ocean University of China* 17: 941–946.

Wilber D and Clarke D (2010) Dredging activities and the potential impacts of sediment resuspension and sedimentation on oyster reefs. In: *Proceedings of the western dredging association thirtieth technical conference, San Juan, Puerto Rico*. Western Dredging Association, pp.61–69.

Yankson K (1990) Preliminary studies on the rearing of the West African mangrove oyster, Crassostrea tulipa, in the laboratory. *Discovery and Innovation* 2(4): 45–51.

Zhu X, Qiang L, Shi H et al. (2020) Bioaccumulation of microplastics and its in vivo interactions with trace metals in edible oysters. *Marine Pollution Bulletin* 154: 111079.

Zu Ermgassen PSE, Bonačić K, Boudry P et al. (2020) Forty questions of importance to the policy and practice of native oyster reef restoration in Europe. *Aquatic Conservation Marine and Freshwater Ecosystems* 30(11): 2038–2049.